Science of the Total Environment 768 (2021) 144370

Contents lists available at ScienceDirect

Science of the Total Environment

journal homepage: www.elsevier.com/locate/scitotenv

Greenhouse gases and biogeochemical diel fluctuations in a high-altitude wetland

Verónica Molina [a,b], Yoanna Eissler [c,*], Camila Fernandez [d,e,f], Marcela Cornejo-D'Ottone [g], Cristina Dorador [h,i], Brad M. Bebout [j], Wade H. Jeffrey [k], Carlos Romero [l], Martha Hengst [i,m]

[a] Departamento de Biología, Observatorio de Ecología Microbiana, Facultad de Ciencias Naturales y Exactas, Universidad de Playa Ancha, Avenida Leopoldo Carvallo 270, Playa Ancha, Valparaíso 2340000, Chile
[b] HUB Ambiental UPLA, Universidad de Playa Ancha, Avenida Leopoldo Carvallo 200, Playa Ancha, Valparaíso 2340000, Chile
[c] Instituto de Química y Bioquímica, Facultad de Ciencias, Universidad de Valparaíso, Gran Bretaña 1111, Playa Ancha, Valparaíso 2360102, Chile
[d] Sorbonne Universités, UPMC Univ Paris 06, CNRS, Laboratoire d'Océanographie Microbienne (LOMIC), Observatoire Océanologique, de Banyuls sur Mer, F-6665 Banyuls/mer, France
[e] Interdisciplinary Center for Aquaculture Research (INCAR), PIA CONICYT COPAS SUR-AUSTRAL Program, Barrio Universitario s/n, Universidad de Concepción, Concepción 4030000, Chile
[f] Centro Fondap IDEAL, Universidad Austral de Chile, Independencia 631, Valdivia 5110566, Chile
[g] Escuela de Ciencias del Mar e Instituto Milenio de Oceanografía, Pontificia Universidad Católica de Valparaíso, Altamirano 1480, Valparaíso 2360007, Chile
[h] Laboratorio de Complejidad Microbiana y Ecología Funcional, Instituto de Antofagasta, Departamento de Biotecnología, Facultad de Ciencias del Mar y Recursos Biológicos, Universidad de Antofagasta, Avenida Universidad de Antofagasta s/n, Antofagasta 1240000, Chile
[i] Centre for Biotechnology and Bioengineering, Santiago 8320000, Chile
[j] Exobiology Branch, Ames Research Center National Aeronautics and Space Administration, Moffett Field, CA 94035-0001, USA
[k] Center for Environmental Diagnostics and Bioremediation, University of West Florida, Pensacola, FL 32514, USA
[l] Laboratorio de Teledetección Ambiental, Departamento de Ciencias Geográficas, Facultad de Ciencias Naturales y Exactas, Universidad de Playa Ancha. Avenida Leopoldo Carvallo 270, Playa Ancha, Valparaíso 2340000, Chile
[m] Departamento de Ciencias Farmacéuticas, Facultad de Ciencias, Universidad Católica del Norte. Av Angamos 0610, Antofagasta 1270709, Chile

HIGHLIGHTS

- Ponds represent a significant landscape in this high-altitude wetland, covering 238 Ha, i.e., 62.4% of the flooded areas.
- Weather conditions including solar radiation, temperature and wind velocity influence biogeochemical diel dynamics.
- Microbial community structure and activity respond to changes mainly associated with nutrients and dissolved organic matter.
- Changes between consecutive days indicate keystone microbial communities, such as Woesearchaeia and Verrucomicrobia.
- This high-altitude wetland produced a net sink for CO_2 and N_2O, and a source of CH_4 in the pond.

GRAPHICAL ABSTRACT

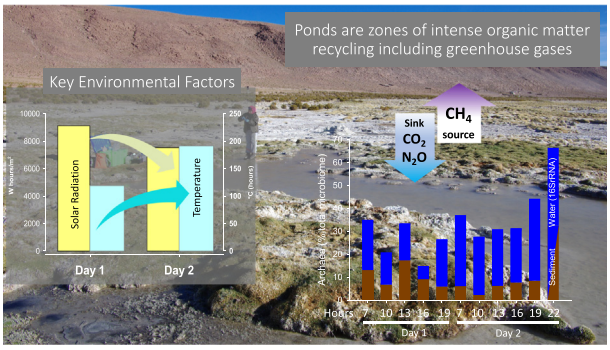

ARTICLE INFO

Article history:
Received 9 September 2020

ABSTRACT

The landscapes of high-altitude wetland ecosystems are characterized by different kinds of aquatic sites, including ponds holding conspicuous microbial life. Here, we examined a representative pond of the wetland landscape

* Corresponding author.
E-mail addresses: veronica.molina@upla.cl (V. Molina), yoanna.eissler@uv.cl (Y. Eissler), camilafernandez@oceanografia.udec.cl (C. Fernandez), marcela.cornejo@pucv.cl (M. Cornejo-D'Ottone), cristina.dorador@uantof.cl (C. Dorador), brad.m.bebout@nasa.gov (B.M. Bebout), wjeffrey@uwf.edu (W.H. Jeffrey), cromero@upla.cl (C. Romero), mhengst@ucn.cl (M. Hengst).

https://doi.org/10.1016/j.scitotenv.2020.144370

Received in revised form 2 December 2020
Accepted 4 December 2020
Available online 30 December 2020

Editor: Frederic Coulon

Keywords:
Greenhouse gases
Diel dynamics
Bacteria
Archaea
High-altitude wetland
Microbial diversity
C and N biogeochemical cycles

for dynamics of greenhouse gases, and their association with other relevant biogeochemical conditions including diel shifts of microbial communities' structure and activity over two consecutive days. Satellite image analysis indicates that the area of ponds cover 238 of 381.3 Ha (i.e., 62.4%), representing a significant landscape in this wetland. Solar radiation, wind velocity and temperature varied daily and between the days sampled, influencing the biogeochemical dynamics in the pond, shifting the pond reservoir of inorganic versus dissolved organic nitrogen/phosphorus bioavailability, between day 1 and day 2. Day 2 was characterized by high dissolved organic nitrogen/phosphorus and N_2O accumulation. CH_4 presented a positive excess showing maxima at hours of high radiation during both days. The microbial community in the sediment was diverse and enriched in keystone active groups potentially related with GHG recycling including bacteria and archaea, such as Cyanobacteria, Verrucomicrobia, Rhodobacterales and Nanoarchaeaota (Woesearchaeia). Archaea account for the microbial community composition changes between both days and for the secondary productivity in the water measured during day 2. The results indicate that an intense recycling of organic matter occurs in the pond systems and that the activity of the microbial community is correlated with the availability of nutrients. Together, the above results indicate a net sink of CO_2 and N_2O, which has also been reported for other natural and artificial ponds. Overall, our two-day fluctuation study in a representative pond of a high-altitude wetland aquatic landscape indicates the need to explore in more detail the short-term besides the long-term biogeochemical variability in arid ecosystems of the Andes plateau, where wetlands are hotspots of life currently under high anthropogenic pressure.

1. Introduction

Wetlands are sites of intense biogeochemical activity including aerobic and anaerobic microbial processes resulting in high greenhouse gases (GHG) recycling. In fact, wetlands constitute one of the greatest natural methane sources in temperate and tropical zones, c.a. 72%, Wuebbles and Hayhoe (2002). However, the magnitude of the GHG wetland budgets, exchange, and direction (net source (emission) or net sink) occur with temporal dynamics. For example, He et al. (2014) reported a seasonal scale associated with temperature and precipitation variability and GHG have been shown to change seasonally in association with temperature and water content in soil samples (Barba et al., 2019). Short-term variability in daily (and diel cycles) could significantly influence GHG fluxes associated with key processes, such as photosynthesis. For example, CO_2 emissions are lower during day versus nighttime, while N_2O and CH_4 showed the opposite pattern in mangrove wetlands (Huang et al., 2019). Long-term warming experiments in artificial ponds indicate greater emissions of CH_4 at night compared with the day. During these 11 years of experimental warming, CH_4 increments were associated with temperature, and with the methanogen versus methanotrophic microbial community structure/activity changes in the ponds (Zhu et al., 2020).

Microbial communities which mediate biogeochemical processes, could be abundant, less frequent and rare, or fluctuate between each category through time (Campbell et al., 2011; Fuhrman et al., 2015). These shifts associated with the structure of the microbial community have been associated with bottom-up controls through substrate availability and top-down control through viral-lysis and grazing. Other environmental conditions that could favor some communities over others include photoinhibition (Campbell et al., 2011; Needham et al., 2013; Smith et al., 2014). Bottom up controls have been shown to stimulate growth and generate pulses in abundance of some microbial groups over short time scales, such as daily and diel cycles (Bunse and Pinhassi, 2017).

On the other hand, the activity of some microbial members of the community exhibit diel rhythmicity in response to day and night cycles as a strategy to optimize their metabolisms. For example, Cyanobacteria, Proteobacteria and Bacteroidetes have a molecular timing mechanism known as the circadian clock (Hörnlein et al., 2018; Johnson and Egli, 2014; Loza-Correa et al., 2010). In a diel cycle study, several functional genes allowed microorganisms to synchronize their biological clocks by light, temperature, or metabolites from neighboring species (Johnson and Egli, 2014). This circadian system, especially in cyanobacteria, is composed of transcriptional and non-transcriptional oscillators that are coupled to promote resilience (Johnson and Egli, 2014). Moreover, nitrogen fixation by non-heterocystous cyanobacteria has been reported to occur mainly during the night in microbial mats, depending on photosynthetic product storage during the day (Bebout et al., 1993; Stal and Heyer, 1987). To date, studies of microbial community composition dynamics over the time scales of a day have been carried out mostly in marine ecosystems and wetlands (Fuhrman et al., 2015; Huang et al., 2019) but to a lesser extent in extreme ecosystems, for example in hypersaline lakes (Andrade et al., 2015).

Salar de Huasco, is an extreme wetland located at 3800 m a.s.l. (above sea level), characterized by diverse aquatic sites such as freshwater springs, streams and isolated ponds with variable salinity. This wetland includes a main shallow lagoon or lake which is permanently present but with a variable area between 175 and 538 km^2 (Dorador et al., 2020). It is inhabited by conspicuous microbial life and is a hotspot of highland fauna (Dorador et al., 2013). Small-scale spatial variability studies showed that microbial community structure at Salar de Huasco was variable in the different aquatic sites, for example showing a higher diversity in the isolated ponds than in the lagoon (Aguilar et al., 2016; Eissler et al., 2019). In addition, high diversity and complexity were observed in ponds holding microbial mats when compared to water sources (springs or lagoons; Eissler et al., 2019). On a synoptic scale, two ponds situated contiguously varied significantly in their dissolved organic carbon (DOC) concentration (from 33.5 to 424.1 mg l^{-1}) and with associated differences in dominant bacterial communities, i.e., Proteobacteria and Bacteroidetes versus Cyanobacteria (Aguilar et al., 2016). The microbial activity in this ecosystem is characterized by high rates of primary productivity (de la Fuente, 2014) and secondary productivity (Hernández et al., 2016), as well as high nitrogen uptake and remineralization (Molina et al., 2018a). In addition, the microbial community activity and contribution to nutrient and GHG recycling could vary in the different aquatic sites and over diel cycles (de la Fuente, 2014; Molina et al., 2016; Molina et al., 2018b). Short term experiments associated with GHG exchange in the main spring area of Salar de Huasco indicate that these areas were characterized by a net sink of N_2O, while CH_4 and CO_2 were released into the atmosphere in both wet and dry seasons (Molina et al., 2018b). Moreover, shifts in the active microbial community composition have been associated with high solar radiation and temperature changes in microcosm experiments conducted at spring sites of Salar de Huasco (Molina et al., 2016). These changes resulted in a reduced activity of Cyanobacteria and other abundant microorganisms as measured using 16S rRNA during the hours of high solar radiation while less abundant and rare groups were relatively more active and therefore had a relatively larger impact on nutrient recycling (Molina et al., 2016). Salar de Huasco represents a model ecosystem of highland wetlands of the Central Andes with still low human impact activities, thus ideal to study natural microbial communities' response to drastic diel changes

in their physical environment such as solar radiation, temperature, wind field (intensity and direction) and their resulting contribution to biogeochemical cycles. In the present study, ponds were selected as representative systems of evaporitic zones where intense recycling of inorganic and organic dissolved compounds, including GHG, is expected in the wetland based on previous reports. We hypothesize that in the ponds, changes in solar radiation through the day will be the predominant environmental factor generating significant changes in the activity of the microbial community within the pond resulting in different biogeochemical conditions in the water column, including high diel GHG production.

2. Materials and methods

2.1. Sampling site and physicochemical variables

The diel cycle sampling was conducted at Salar de Huasco during November 2015, at the site H3, (20°16.98′S, 68°53.33′W, see Fig. 1A). Sampling started at 07:00 h with samples being taken every 3 h until 19:00 h and 22:00 h local time on November 9th and 10th, respectively. The surface water of the pond froze during the night; thus sampling for both days was not possible after the timepoints mentioned. The pond sampled covered an area of 68.98 m^2, was 15 cm deep, and was characterized by soft bottom sediment with a few spots of disassociated microbial mats (Fig. 1B, Fig. S1). Solar radiation, air temperature and wind velocity were downloaded from http://www.ceazamet.cl/index.php?pag=mod_estacion&e_cod=SALH&p_cod=ceazamet recorded with a Meteorological station (Campbell Scientific Inc.) located at approximately 3 km from the sampling site (Fig. S1). A combination of unmanned Aircraft System (UAS) and satellite images downloaded from Landsat and Sentinel, were used to generate a study area map (dates used, November 19th, 2015 and March 15th, 2019 from Landsat 8 and Sentinel 2, respectively). The UAS images were corrected (orthorectification) and processed for geo referencing using Software Pix4D. In addition, the flooded area of the wetland was estimated for contrasting seasons using multispectral images with the software ArcGis 10.4.

Physicochemical variables, conductivity, temperature, pH and dissolved oxygen, were measured in situ in the water column using a portable Thermo Scientific Orion Star Multiparameter Meter (model A329). Water samples for determining ammonium concentration were collected in triplicate directly into Duran Schott flasks (50 ml) and immediately processed following the fluorometric method (Holmes et al., 1999). Fluorescence for ammonium estimations were measured using a Turner Design fluorometer in the field and the detection limit determination was 0.01 μM. Water for nitrate, nitrite and phosphate determination were collected in triplicate, filtered through a GF/F filter (Whatman) and stored in rinsed Nalgene flasks (125 ml). These samples were frozen in the field and stored at −20 °C until analysis in the lab. Nutrient samples were analyzed using standard colorimetric methods with an automatic nutrient analyzer (Atlas et al., 1971).

Samples for dissolved organic nitrogen and phosphorus (DON, DOP) (30 ml, in triplicates) were filtered through pre-combusted (450 °C, 6 h) GF/F filters (Whatman) and the filtrates were stored in Teflon bottles. These samples were analyzed using the wet-oxidation method (30 min, 120 °C) following Pujopay and Raimbault (1994). Dissolved organic carbon was collected in pre-combusted (450 °C, 6 h) glass ampoules acidified with H_3PO_4 (85%) and stored in the dark at 4 °C. These samples were analyzed in a high-temperature combustion on a Shimadzu TOC-L analyzer at Laboratoire d'Océanographie Microbienne, LOMIC (Banyuls Sur Mer, France).

Water samples (50 ml) for H_2S determinations were collected using a 60 ml syringe by gentle filling into falcon tubes (avoiding bubbles), fixed with $ZnCl_2$ (2 ml, solution 5 mM) and kept refrigerated until analyses, following the specifications of the spectrophotometric method developed by Cline (1969). The limit of detection of the analyses was 0.06 μM.

2.2. Greenhouse gases determinations

Triplicate discrete water samples were collected for GHG determination using 20 ml vials, fixed with 50 μl of saturated mercuric chloride avoiding bubbles and stored in the dark. Before chemical analysis, a headspace was generated using ultrapure Helium gas following (McAuliffe, 1971). After equilibrium, a headspace gas sample was analyzed in a gas chromatograph (GC-2014 Greenhouse, Shimadzu) equipped with an electron capture detector (ECD) for N_2O, a methanizer for CO_2 conversion to CH_4 and a flame ionization detector (FID) for CH_4 determination. Concentration was determined based on a three-point calibration curve with helium, air, and a standard of 600, 5, and 1 ppm for CO_2, CH_4 and N_2O, respectively (Scotty gas mixture; Air Liquid Co).

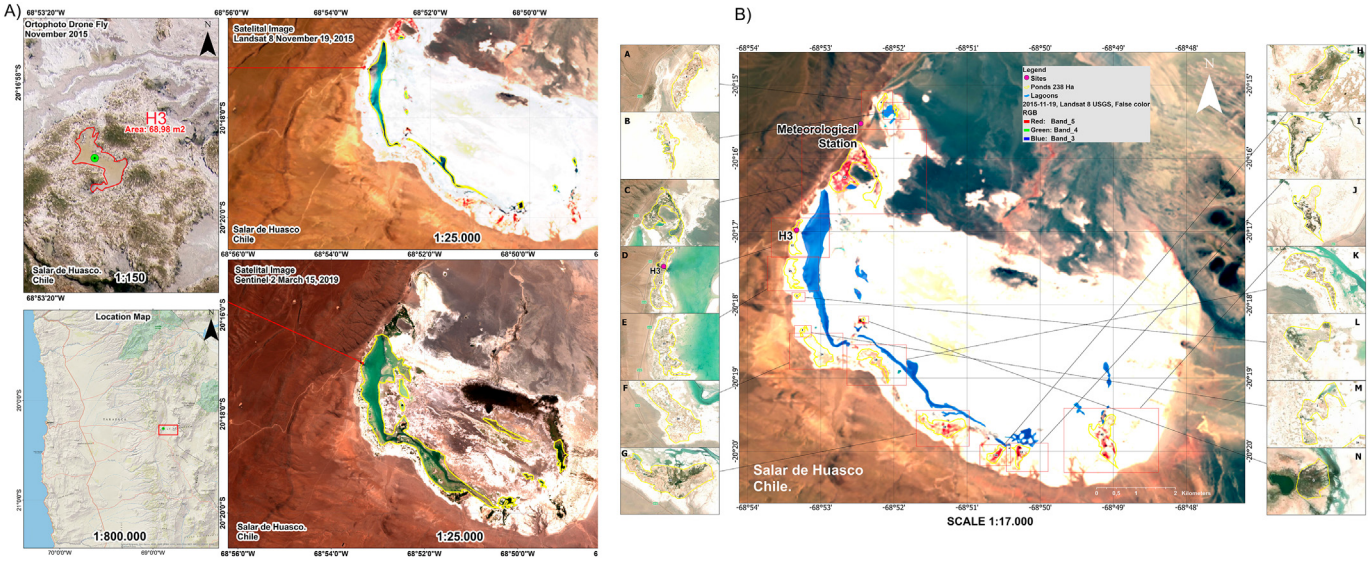

Fig. 1. A) Maps showing the location and area of the site sampled at different scales during the diel cycles and showing the overall look of the wetland during dry season (November 2015, upper panel) in comparison to wet season (March 2019, bottom panel). B) Map layouts showing areas of the wetland associated with ponds, the localization of the sampled site (H3) and the meteorological station.

GHG excess was determined by the difference between the expected GHG concentrations in equilibrium, considering the measured temperature and conductivity, and the water concentration. Net fluxes were estimated based on the differences between each sampling point, then summed and dividing it with the number of hours of the two diel cycles. To upscale our estimations, the fluxes estimated here were transformed first from μmol l^{-1} h^{-1} to mmol m^{-3} d^{-1}, and then to mg m^{-2} d^{-1} and Kg d^{-1}, considering the molecular weight of each gas, an average depth (0.1 m) and the total landscape area covered by ponds 2,380,000 m^2 (238 ha).

Flux chamber experiments were performed to determine the flux of greenhouse gases across the sediment-water interface during the second day (November 10th). The flux chambers have a central stirring paddle to homogenize the water and sampling ports with septa for water and gasses through a headspace and were deployed following Canfield and Des Marais (1993). Five chambers were installed at 10:30–11:30 h and were incubated during seven hours. Gases samples were removed from the headspace at three time points (12:00 h, 14:00 h and 19:00 h). Rates were estimated using linear regression considering $R^2 > 0.5$ and typical error. The rates in ppm (CO_2 and CH_4) and ppb (N_2O) per hour were transformed considering the standard density of each gas (mass per m^3), the molecular weight and then upscaled as described for discrete water analyses.

2.3. Microbial communities sampling

Water samples to determine picoplankton abundance were collected in replicate cryovials (1 ml), immediately fixed with glutaraldehyde (0.1% final concentration), and stored frozen in liquid nitrogen until analysis. Total picoplankton abundance was estimated through flow cytometry (FCM) using a FAC- SCalibur flow cytometer (Becton Dickinson) equipped with an ion–argon laser of 488 nm of 15 mW, following the method described by Marie et al. (1997). Water and sediment samples were collected to study microbial community composition for subsequent metabarcode (iTag) 16S rRNA and rDNA sequencing. Microbial communities from surface sediments were sampled with a sterile spatula and approximately 500 μl placed into cryovials. The water column microbial community was concentrated in the field by filtration onto a filter (0.22 μm hydrophilic PVDF filters, GVWP02500, Millipore) using a Swinnex filter holder (25 mm diameter) attached to a syringe (60 ml). Both sediment and water biological samples were placed in cryovials with RNAlater solution (Ambion, Life Technologies, USA) and then stored at −80 °C until analysis.

2.4. Secondary production

Experiments to determine ^{3}H-leucine incorporation into bacteria and archaea biomass (microbial secondary production, MSP) were carried out during day 2 following Hernández et al. (2016). Total microbial secondary production and the contribution of archaea to secondary productivity were determined after the addition of N1-guanyl-1,7 diaminoheptane GC7 (0.4 mM) an hypusination inhibitor affecting archaea cell cycle (Jansson et al., 2000) and used before (e.g., Levipan et al., 2007). Incubations were conducted in 2 ml microcentrifuge tubes. Triplicate 1 ml were added to tubes containing ^{3}H-leucine (10 nM final concentration) or ^{3}H-leucine+GC7. A T0 control was amended with trichloroacetic acid (TCA, 5% final *v*/v) prior to incubation. Samples were incubated for approximately 2 h at in situ temperature. Incorporation was terminated by the addition of TCA (final 5% v/v). Samples were stored refrigerated in the dark until processing using a microcentrifuge method of Simon and Azam (1989) and a Packard Model 1600TR liquid scintillation counter. Rates estimations were expressed as μg C l^{-1} h^{-1} using the 0.86 ratio of cellular carbon to protein and 0.073 for leucine (Simon and Azam, 1989).

2.5. Microbial community analyses

To evaluate the active microbial community structure, RNA was extracted from sediments and the water. RNA was extracted using an Ambion RNA extraction kit (AM1560) according to manufacturer's protocol with the addition of a mechanical disruption step with 200-μm-diameter zirconium beads (Low Binding Zirconium Beads, OPS Diagnostics) for two rounds of 30 s (~3000 rpm) using a Mini-Beadbeater-8TM (Biospec Products). DNA and RNA quantification were determined by fluorescence using a Qbit 2.0 instrument. For RNA analyses, DNA was removed using the TURBO DNA-*free*™ kit (Invitrogen) and RNA was tested for residual DNA by standard bacterial 16S rRNA amplification. RNA was reverse-transcribed with random primers provided by the ImProm-II™ Reverse Transcription System (Promega Corp.). DNA was also extracted from sediment samples using PowerSoil DNA Isolation Kit (MoBio Laboratories) following the manufacturer's specifications to evaluate the present community as additional information for this biome. The bacterial 16S rRNA gene was sequenced using the primer 27F (5′-GAGTTTGATCNTGGCTCAG-3′) in combination with 519R (5′-GTNTTACNGCGGCKGCTG-3′), and for archaea the primers Arch349F (5′-CCCTAYGGGGYGCASCAG-3′) combined with Arch806R (5′-GGA CTA CVS GGG TAT CTA AT-3′) were used. Sequencing was carried out using a high-throughput Illumina Miseq at Mr. DNA sequencing service. The resultant 16S rRNA and rDNA gene sequences were processed using the Mothur software v1.35.1 (Schloss et al., 2009). Reads < 200 bp were deleted and sequences that contained more than one undetermined nucleotide (N) and those with a maximum homopolymer length of 8 nucleotides were trimmed. UCHIME algorithm was used to identify and remove chimera sequences (Edgar et al., 2011). The retrieved 16S rRNA and rDNA gene sequences were classified taxonomically using the automatic software pipeline SILVAngs available at https://www.arb-silva.de/https://www.arb-silva.de/ based in a ≥ 93% of alignment identity according to Quast et al. (2013). The number of samples sequenced ($n = 66$) were deposited in the European Nucleotide Archive (ENA) under accession Nr. PRJEB31701 (ERS3230768 - ERS3230839).

2.6. Environmental and microbial community statistical analysis

A Spearman rank correlation was performed to understand the relationship among environmental variables and the Mann-Whitney *U* Test to check differences between these variables during the two different days of the experiment using Statistica version 7.0 software. To facilitate the visualization of different units and magnitudes, data log-transformation was estimated and then the difference between each point and the average ($n = 11$) of both days was graphed.

Principal component analysis (PCA) was used to evaluate the influence of physical and chemical variables studied along the two diel cycles. Principal coordinates analysis (PCoA) were used to visualize microbial community changes from the different biomes along the diel cycle. Bray Curtis similarities were first estimated using square-root transformed data. The contribution of the different taxa (Phyla level and OTU) to dissimilarity associated with day 1 and 2 (as factor) was estimated using Similarity Percentages-species contributions (SIMPER analyses). Distance-based linear models (DISTLM) were estimated from resemblance matrices, using 9999 permutations with Akaike Information Criterion (AIC), using the present and active microbial community combining the two days. PCA, PCoA and DISTLM were estimated using the software PRIMER (7.0.11) with the PERMANOVA add on (Anderson et al., 2008). The microbial community was analyzed using operational taxonomic units (OTU) to obtain richness and Alpha diversity indexes (Shannon (H′) and Pielou's evenness) using PRIMER software. The analyses were compared using One-Way ANOVA. To compare richness oscillation through the day an estimation of a rarefaction richness value was calculated based on normalized sequences (the library with the smaller number of reads was $n = 29{,}000$).

3. Results and discussion

The studied area was characteristic of an evaporitic pond at the H3 site in the Salar de Huasco wetland associated with the dry season (November 2015), situated close to the main lagoon area (see Dorador et al., 2013; Eissler et al., 2019). The H3 sampling area presented many ponds during the month of sampling (Fig. 1B, see small panel D). However, the area could be completely flooded during the wet season (Fig. 1A, March 15, 2019). Satellite images analysis indicates that the flooded area during the sampling year (2015) was on average 351 Ha, whereas during an extreme wet season observed in March 2019 the flooded area could reach 640.9 Ha, shown here as an example of a maximum (Fig. 1A, right bottom panel). Precipitation changes in the high Andean steppe are tightly connected with climate variability such as the interannual ENSO (El Niño Southern Oscillation) and other climatic events (Barrett et al., 2016; Houston, 2006).

Ponds are characteristics of Andean wetlands, some of them present diverse and seasonally growing peatland vegetation depending on water availability. The type of peatland vegetation is usually related to springs presence, precipitation, and conductivity (Squeo et al., 2006). The pond studied here (H3 site) was characterized by a shallow water layer (c.a. 0.15 m depth) covering an area of 68.98 m^2, representing a total volume of 10,347 l. This pond was considered as a model of evaporitic aquatic areas of the wetland. In fact, using satellite image analyses we determined that the total area covered by ponds during the month of sampling represented c.a. 238 Ha, similar in magnitude to main lake (Fig. 1B). Thus, our experiment provided valuable information into the role of pond biogeochemical diel dynamics associated with extreme climatic variability in the highlands of the Chilean desert.

3.1. Environmental variables and biogeochemical dynamics in two contrasting diel cycles

The meteorological conditions during day 1 and day 2 were variable during the day and were characterized, respectively, by an average (± SD) of 384±460 versus 315±407 W m^{-2} and an integrated irradiance of 9113 and 7516 W h m^{-2} (solar day, 14 h), 5.0±8.5 versus 8.1±5.8 °C (air temperature) and 2.7±2.0 versus 2.8±1.7 m s^{-1} (wind velocity), Fig. 2. Day 2 received less solar radiation, higher wind velocities and temperature particularly before noon compared with the previous day, differences that were not statistically significant (Mann-Whitney *U* Test). Air temperature and wind field were variables significantly correlated with changes in water temperature, conductivity, oxygen, pH and other organic and inorganic compounds associated with microbial recycling processes such as total dissolved nitrogen (TDN), NH_4^+ and H_2S (Table S1).

The water biogeochemical conditions were plotted in Fig. S2. In general, the pond was characterized by oligosaline (2169–2655 μS cm^{-1}) and alkaline conditions (pH 9.19–9.38), but variable temperature and dissolved inorganic and organic compounds, including greenhouse gases changing through the day and between the sampling days. The water temperature varied between 1.5 and 20.5 °C showing lower values in the morning, mainly at day 1. During day 1, phosphate, nitrite and silicic acid presented maxima during the morning, whereas ammonium presented a maximum during the afternoon and evening. During day 2, phosphate and silicic acid were more homogeneous, whereas nitrite decreased, and ammonium was more variable than day 1. DOC presented higher concentrations during day 1, decreasing towards the evening, whereas the opposite was found during day 2. TDN presented homogeneous concentrations during day 1 and higher concentrations during day 2, reaching a maximum value at 19:00 h. A similar trend was observed for total dissolved phosphorus (TDP) but reaching a maximum at 13:00 h (day 2). CO_2 was lower during noon and hours of high solar radiation during both samplings (between 10:00 h and 13:00 h), whereas the opposite was found for CH_4 and N_2O. However, N_2O reached maxima concentration during day 2. The variability present

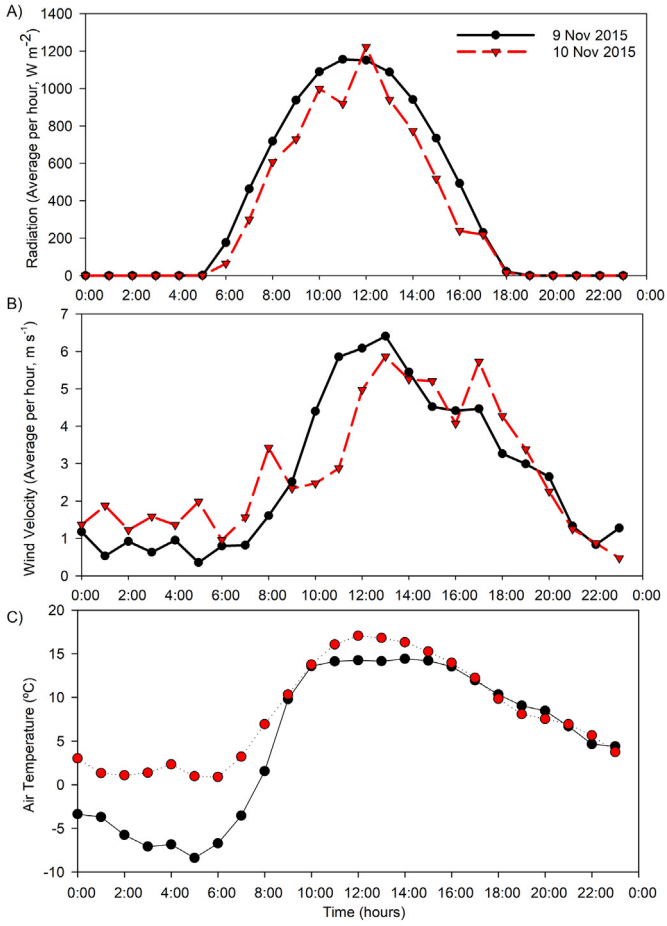

Fig. 2. Averages per hour of A) solar radiation, B) wind velocity and C) air temperature registered in the meteorological station during diel cycles of November 9th and 10th, 2015.

for both days was clearly observed when differences from the total average were calculated (Fig. 3). This suggests that most of the variables presented shifts (increase versus decrease compared with the average) associated with solar radiation (10:00–13:00 h) and water temperature (13:00–16:00 h; Fig. 3). Moreover, the magnitude of the trends was high for some, such as DOC and nutrients during day 1 compared with day 2 and TDP and TDN and N_2O during day 2, differences supported by Mann-Whitney U Test ($p < 0.05$). In fact, principal component analysis (PCA, Fig. S3) indicates that the variables studied accounted for 52.3% of the variability, PC1 was associated with temperature (air and water), wind velocity and other physical and chemical conditions in the water, whereas, PC2 was associated with dissolved organic matter mainly nitrogen (DOC:DON, TDP).

The GHG excess variability was associated with temperature and solar radiation changes (Fig. 4). During the morning, CO_2 and N_2O were undersaturated (negative values), whereas during the afternoon both were supersaturated (positive values) in the water of the pond. On the other hand, CH_4 was always supersaturated in the water. The estimated net budget (sum of all excess values) indicates that the pond was characterized by CH_4 production, whereas CO_2 and N_2O were consumed by biological processes. This result was supported by correlations of CO_2 and N_2O excess with NH_4^+ and DOC (Spearman Rank $R > 0.63$, $p < 0.05$ and < -0.61, $p < 0.05$, respectively, Table S1). The morning CO_2 undersaturation suggests its fixation by autotrophic microorganisms, including photosynthetic processes in the pond. This active community could also explain the decrease of nutrients observed at similar hours during day 1 (Fig. S2). Considering nutrients temporal accumulation or disappearing through time during the morning and

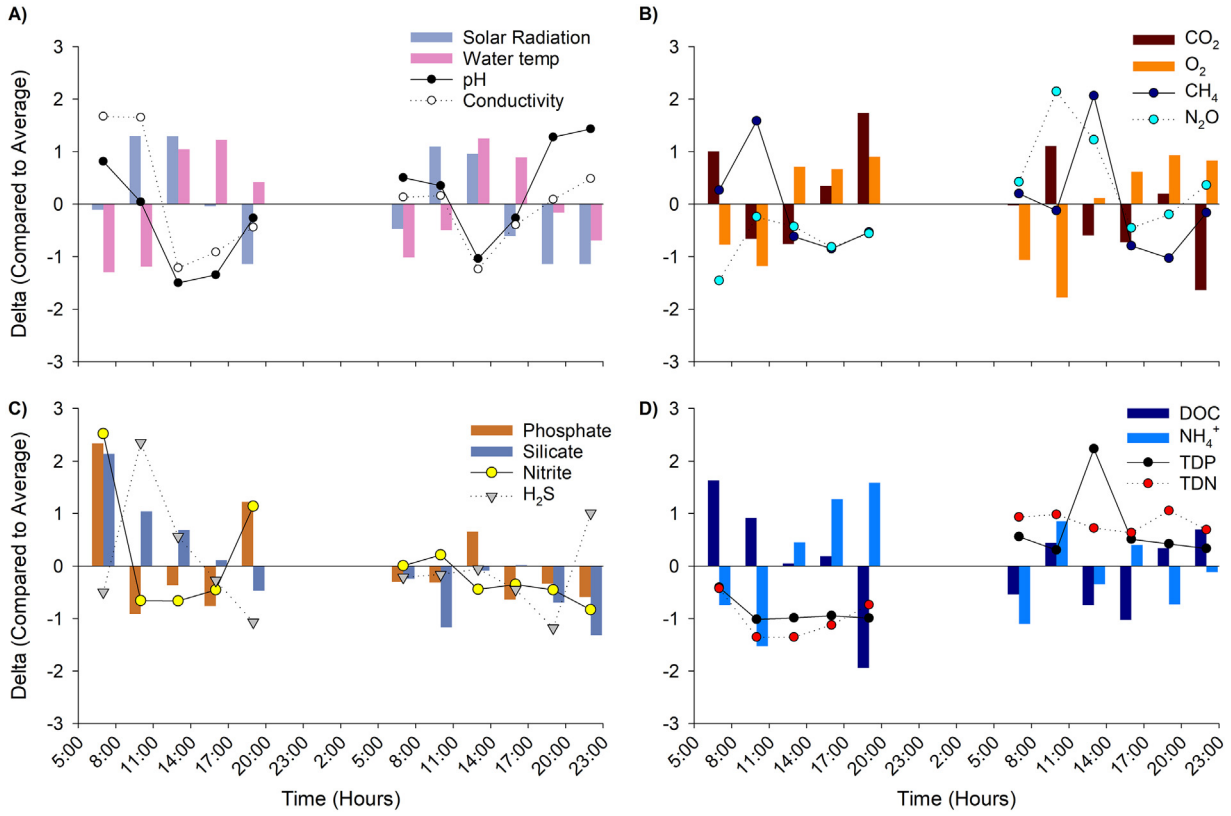

Fig. 3. Plot showing tendencies of physical and chemical variables during both diel cycles considering A) solar radiation, temperature, pH and conductivity, B) GHG and oxygen, C) inorganic nutrients and hydrogen sulfide and D) dissolved organic carbon, nitrogen and phosphorous and ammonium. The average was the data retrieved for both days ($n = 11$ for each variable).

afternoon, rates of change were determined when a linearity $R^2 \geq 0.6$ was estimated (Table S2). For example, the ammonium and nitrite rates of change observed during day 1 were in similar magnitudes than potential nitrogen demand by the microbial community including nitrification rates in the study area (Molina et al., 2018a).

The CO_2 excess estimation observed during day 2 was lower than the previous day (an average of −4.5 versus −8.7, Fig. 4) particularly at 10:00 h, probably due to a lower radiation received before 10:00 h compared with the previous day (of 100 W m^{-2} and a total exposure difference of 1597 W h m^{-2}). In addition, during day 2 a high wind velocity was observed before 10:00 h, expected to generate a higher mixing than the previous day in the shallow water pond (Fig. 2). Wind velocity was a variable correlated significantly with water physical and chemical parameters such as water temperature, pH and conductivity (Table S1). The increment of wind stress could reduce the photosynthetic activity,

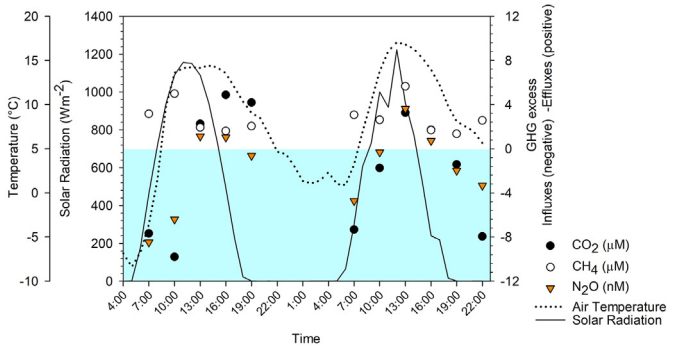

Fig. 4. GHG excess and its association with air temperature and solar radiation. Negative value of excess indicates a consumption (sink) and a positive value indicates a production (source).

and potentially other processes in this system, through sediment resuspension and solar radiation attenuation (de la Fuente, 2014). In total, considering the negative CO_2 excess (Fig. 4) as a "net primary productivity rate per day" the autotrophic incorporation of carbon varied between 0.3 and 1.7 g C m^{-2} d^{-1}. In the pond area, these rates were comparable with benthic primary productivity (0.6–1.54 g C m^{-2} d^{-1}) estimated previously in sediments for the main lake of Salar de Huasco modeling heat and oxygen fluxes using microprofiles (de la Fuente, 2014). These values in terms of CO_2 fluxes were comparable with other shallow terrestrial ecosystems including ponds (Torgersen and Branco (2008).

The CO_2 positive excess observed during the afternoon (13:00–16:00 h) of both days could be indicative of respiration processes and suppression or decrease of photosynthesis. During the afternoon of day 1, the excess reaches greater and consistent positive values, increasing between 2.3 to > 4.2, whereas during day 2, these values were mostly negative (Fig. 4). High irradiance has been reported to inhibit photosynthesis and decrease CO_2 fixation rates through the process known as photoinhibition (e.g., review by Long et al., 1994). While it is possible that this occurs between 10:00 and 13:00 h during both days, the effect appears greater during day 1 associated with higher solar radiation observed in the morning hours (Fig. 2). In addition, the decrease in solar radiation and high temperature might enhance respiration in the afternoon (13:00–16:00 h). The combined effect of both high respiration processes and the suppression or decrease of photosynthesis may be responsible for increases in ammonium, nitrite, TDN, phosphate, and organic matter consumption that were observed concomitantly in the pond (Table S2, Fig. S2). Substrate competition between photoautotrophs and microorganisms with heterotrophic and chemoautotrophic metabolisms have been reported to impact aquatic microbial activities and have effects on diel variability in marine ecosystems (Fuhrman et al., 2015; Kuipers et al., 2000;

Smith et al., 2014). In contrast to marine ecosystems, extreme high-altitude environments may have mechanisms favoring heterotrophic or chemoautotrophic activity that could also involve a significant reduction in substrate competition due to photoautotrophic photoinhibition at hours of high radiation and a rate decrease due to lower irradiances in the afternoon (>16:00 h). However, the photo – physiological plasticity of the photosynthetic organisms in the pond of Salar de Huasco should be further explored, for example, using isolates as in Prelle et al. (2019) or in-situ using effective and maximal quantum yield (Fv/Fm) approaches (Figueroa et al., 2014; Sawall and Hochberg, 2018).

Short term flux measurements performed using chambers during the afternoon of day 2 indicate that the sediments are the main GHG source in the pond reservoir (Fig. S4 and S5; Table S3). However, positive GHG accumulation rates in the headspace chamber were more consistently observed for CH_4 than other gases, whereas CO_2 and N_2O accumulate in lower rate and probably recycled in the sediment (for example by methanogenesis that uses CO_2 as substrate). CH_4 and CO_2 concentrations in the flux chambers averaged 60–70% higher than discrete water determinations measured during the afternoon. If our measurements in the water indicate a net balance of GHG recycling in the pond, then it is possible that a similar percentage is consumed by planktonic microbial communities and/or escape directly into the atmosphere through bubbles (ebullition). Direct ebullition could be an important CH_4 source from wetland soil from peat bogs (Tokida et al., 2005) and small water bodies such as ponds (Grinham et al., 2018). However, the concentration of GHG accumulated in the headspace of our chambers were lower compared with previous GHG determination from bubbles trapped underneath well-developed microbial mat matrix, i.e., CH_4 and CO_2 were in average 59,054 and >3839 ppm, respectively (Molina et al., 2018b).

Ponds, whether natural or manmade associated with farming activities and urban areas, are considered as important sites of carbon burial (Smith et al., 2002) and could be numerically significant in a global scale (Downing et al., 2006). The pond studied here in a high-altitude wetland could also be considered as a site of intense organic matter recycling and contributing to the GHG budget as a representative of a typical landscape of the Andes plateau basin. The estimated GHG exchange fluxes for CO_2, N_2O and CH_4 reached respectively, 226, 0.115 and 10.3 mg m^{-2} d^{-1} in the pond sediment and −17, −0.007 and 689 mg m^{-2} d^{-1} in the pond water (Table S3). These diel GHG fluxes per area were upscaled to evaluate the potential contribution of the pond areas landscapes determined to be 238 Ha using satellite images analyses and an average depth of 0.1 m of water, and could represent 603, 0.44 and 24 kg d^{-1} and -40.9, −0.017 and 1649 kg d^{-1} for the pond sediment and water (Table S3). The magnitude of fluxes was in the range of water-atmosphere fluxes determined in different aquatic areas of the Salar de Huasco wetland (Molina et al., 2018b) and, in general, were in the lower range for CO_2 and N_2O and in the range of CH_4 compared with other aquatic ecosystems including high-altitude wetlands (see Table S4).

However, unlike the spring aquatic site flux chamber diel experiment carried out previously in the wetland (Molina et al., 2018b), the pond studied here represents a net sink of CO_2. The total contribution of the high-altitude ecosystems to GHG budgets should be further studied considering the potential variability of microbial communities inhabiting different ponds (Aguilar et al., 2016).

3.2. Microbial community dynamics and shifts in the archaea versus bacteria contribution during the diel cycle

Picoplankton cells abundance varied slightly between 1.44 ± 0.09 × 10^4 and 2.00 ± 0.02 cells × 10^4 ml^{-1} with a maximum observed during day 2 at hours of highest irradiation (Table S5). The difference is higher in day 2 as observed in Fig. S4. During this day, microbial secondary production was determined (Fig. 5). These rates also varied through the day, characterized by a maximum at hours of high radiation but low

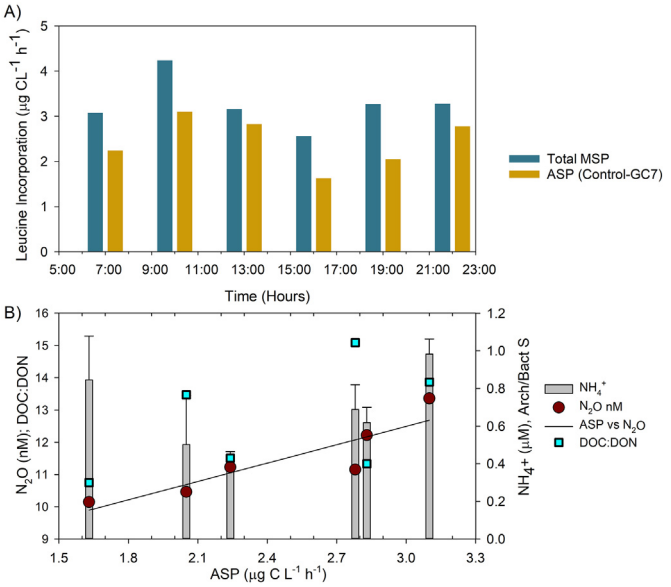

Fig. 5. A) Microbial secondary production (MSP) measured during day 2 (November 10th, 2015) and Archaea secondary productivity (ASP) production estimated from Control- GC7 (N1-guanyl-1,7 diaminoheptane) as inhibitor of archaeal metabolism and B) ASP and its relationship with ammonium, nitrous oxide (linear regression R^2 =0.8, p<0.01) and DOC:DON.

temperature and vice versa (10:00 h and 22:00 h). A large portion of the microbial secondary production (MSP) could be attributed to archaea (62–89%), based on the difference between total MSP and GC7 amended sample. A previous study indicates that isolated ponds, or waterbodies having non-visible surface connection with water streams, hold a highly active microbial community reaching the highest secondary productivity magnitude (0.87–11 µg C l^{-1} h^{-1}), in contrast to spring and streams in the wetland (Hernández et al., 2016).

The MSP was correlated with DOC and DOC:DON and the contribution of archaea to secondary productivity (ASP) was significantly correlated with N_2O (Table S1). These relationships support the importance of substrate availability in the secondary productivity in the pond.. DOC:DON ratio variability is indicative of changes in dissolved organic matter composition and possibly higher nitrogen bioavailability (Yates et al., 2019). Moreover, the relative contribution of both domains in the total retrieved sequences (archaea versus bacteria ratio, mainly in the water) changed during the diel cycles and were correlated with environmental variables (wind and solar radiation) and DON and DOP compounds such as nitrogen and phosphorus, and sediment community ratios with MSP (Fig. 6, Table S1). As with meteorological and chemical variables, differences in the archaea and bacteria ratio from the average were calculated; this analysis helped to visualize shifts in the relative contribution of active domains in the pond between the two days (Fig. 7). On both days, there was a peak of bacterial sequence reads in the water (relative to archaeal) in the early afternoon, followed by a peak in archaeal sequence reads (relative to bacterial) later in the afternoon. A similar pattern was observed in the sediments on the second day, that coincided with higher ASP observed during day 2. The archaeal enrichments in the late afternoon coincided with higher nitrogen availability in the water, NH_4^+ during day 1 and TDN during day 2. These results support recent reports of a connection between archaeal secondary production and TDN in ponds from coastal wetland ecosystems (Batanero et al., 2020). Moreover, the relationships between nitrogen enrichments and archaeal activities could also enhance greenhouse gases production in the afternoon also supported by the positive correlation of ASP and archaea versus bacteria ratio (water) with N_2O (Table S1). This result agreed with reports showing nitrous oxide production by archaea as a consequence of nitrogen fertilization in agricultural soils (Wang et al., 2016). This response has been associated with

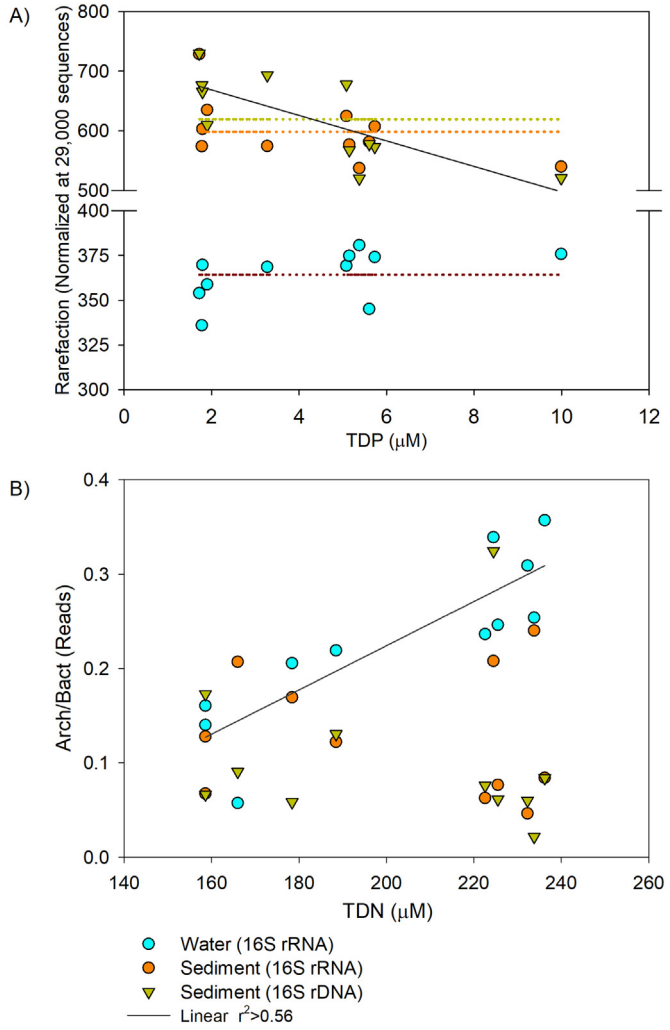

Fig. 6. A) Normalized richness variability compared with average (dotted lines) in the different biomes analyzed associated with solar radiation and B) Archaea versus Bacteria sequencing reads ratio dynamics associated with solar radiation (Water 16S rRNA showing a decreasing tendency). TDP (Total Dissolved Phosphorous) and TDN (Total Dissolved Nitrogen).

Thaumarchaeota, known to use organic compounds such as urea and contribute to N_2O production through ammonia oxidation, the first step of nitrification, in contrasting ecosystems including marine (Löscher et al., 2012) peatlands (Siljanen et al., 2019), and soils (Wang et al., 2016. However, in our study along with some Thaumarchaeota (*Nitrosopumilus and Nitrososphaera*) other functional groups related with nitrification were detected predominantly in sediments, including ammonia-oxidizing bacteria (*Nitrosomonas*) and nitrite-oxidizing bacteria (*Nitrospina* and *Nitrospira*) (Section 3.3) (Fig. S6).

3.3. Microbial community structure changes during the diel cycle

Microbial community structure (present and active 16S rDNA and rRNA, respectively) were slightly variable in the water and sediment during the diel cycle considering rarefied richness and other alpha diversity indexes (Table S6, Fig. S7). In general, the water was characterized by a lower richness and diversity compared with the sediment, which was associated with evenness changes (Fig. S7). In the sediment, 16S rRNA versus 16S rDNA were comparable between each other in day 1 and day 2, but the active microbial community (16S rRNA diversity indexes) was characterized by a higher variability compared with the present community (16S rDNA diversity indexes). In addition, a slight but not significant decrease in both indexes was observed between day 1 and day 2 (Fig. S7). Spearman Rank Correlation analyses (Table S1) using richness indicate that the microbial community, both present (DNA) and active (RNA), were correlated mainly with potential substrates (organic matter, nutrients). Our results support previous studies that showed significant correlation between nutrients, light-turbidity and community structure in lakes (Juottonen et al., 2020). In general, the higher variability within the active fraction compared with the present microbial community in our study supports previous reports using 16S rRNA versus 16S rDNA in natural microbial communities, indicating the relevance of low frequency but highly active OTUs in aquatic ecosystems (Campbell et al., 2011). Some microorganisms associated with low frequency or even undetected OTUs at 16S rDNA (depending on sequencing approach), could respond in a great proportion to perturbations in their environment, such as nutrients inputs or primary productivity variability in time series studies (Campbell et al., 2011; Shade et al., 2014).

DistLM analysis used to explore the relationships of microbial community structure associated with environmental variables suggest that variables such as wind velocity, conductivity, NH_4^+, TDN, N_2O, CH_4, phosphate, H_2S and O_2 account for 70.2% of the sediment present phyla variability (AIC 28.907, R^2 0.99, RSS 24.721), whereas only DOC: DON were associated with the active phyla but with low solution values (AIC 60.069, R^2 0.22, RSS 1799.2). On the other hand, air Temperature, CO_2, DOC, DON: DOP, pH, N_2O, NH_4^+, and CH_4 (AIC 23.967, R^2 0.97, RSS 15.776) account for up to 69.5% of the water phyla diel variability. In total, DistLM analysis indicates that environmental variables associated with meteorological conditions, but also metabolic substrate and products of the microbial community metabolisms, such as nutrients and

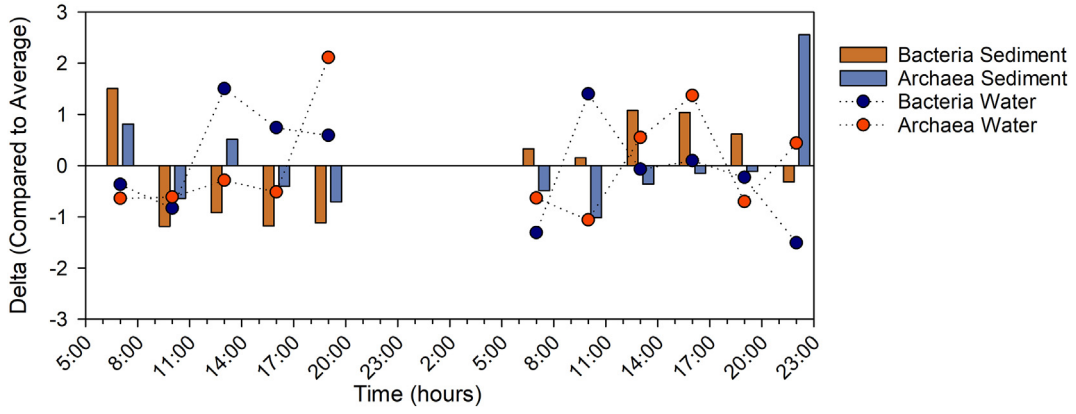

Fig. 7. A) Bacteria and archaea tendency considering differences from the average of both day and microbial taxa presented significant cycling during our experiments in the different compartments and templates.

gases, were relevant in determining the diel biogeochemical distribution in this pond. This result supports previous studies related to bottom-up microbial community control associated with nutrient (nitrogen and phosphorous) pulses and the interaction with photoautotrophic organisms' daytime primary productivity (Kuipers et al., 2000; Smith et al., 2014). In our study, a higher productivity was expected during day 1 (given the greater CO_2 negative excess). Day 1 was characterized by a higher microbial diversity, mainly in the sediments, and higher inorganic nutrients concentration in the water, resulting in increased dissolved organic matter with higher N bioavailability (DOC:DON). In addition, DistLM analysis indicates that different meteorological variables accounted for the microbial dynamics in the water compared with the sediment biome, i.e., air temperature versus wind velocity, respectively. This suggests that the microbial community in sediments could be less sensitive to drastic air temperature changes in Salar de Huasco, but more sensitive to the effect of wind velocity, associated with mixing and turbidity. Diel heat and oxygen micro profiling in the shallow lagoon of Salar de Huasco have shown previously that the sediments absorb solar radiation and heat during the day (de la Fuente, 2014). That study also demonstrated that wind velocity was correlated with the primary productivity layer within the sediment changing from 3 mm to 1 mm under calm versus windy conditions, respectively.

3.4. Active microbial groups and its potential contribution to biogeochemical processes and GHG changes

Microbial composition indicates that a total of 54 phyla were detected, with Bacteria representing by far the most predominant group followed by Archaea and unclassified sequences (<93% identity with databases) in the sediments and water (Figs. S8 and S9). There was little overlap in community composition between the sediment and the water; the two compartments shared <60% similarity. Principal Coordinates Analysis helped to visualize the variability of the microbial community studied, supporting that the active phyla from the water differentiated from the present or active phyla from the sediment (PCoA, Fig. S10). In the sediments, Archaea was dominated by Nanoarchaeota (99% associated with Woesearchaeia) among the seven phyla detected in our study (Fig. S8B), except during the afternoon (day 1) and night (day 2), which were respectively characterized by Thaumarchaeota (up to 71%) and Euryarchaeota from a single order (Methanomicrobiales, up to 68%). In the sediment, bacteria were richer than archaea and were composed by the following abundant phyla: Bacteroidetes (12 orders), Proteobacteria (75 orders, but dominated >24% of Burkholderiales, Rhodospirillales, Desulfovibrionales, Desulfobacterales) and Verrucomicrobia (11 orders; Fig. S8C). The microbial composition in the water (Fig. S9) indicates that archaea was also dominated by Nanoarchaeota (99% associated with Woesearchaeia), except in the evening (19:00 h day 1) where Euryarchaeota from a single class of Halobacteriales contributed up to 93% of the community (Fig. S9). Nanoarchaeota were enriched in its activity during day 2 compared with day 1. In addition, Euryarchaeota from the orders Methanomicrobiales and Methanosarcinales also contributed up to 10% of the community composition. Thaumarchaeota were rare and accounted for ~1% of the total archaea community during the evening of day 1 and early morning of day 2. The active bacteria were more homogeneously distributed in the water, characterized by a dominance of Proteobacteria (61 orders) followed by Bacteroidetes (7 orders; Fig. S9C).

Active OTUs based on 16S rRNA vs 16Sr DNA ratios were estimated with the sediment sequences, the top active groups detected in all the different sampling times were plotted in Fig. 8A, and their water counterparts were plotted (Fig. 8B). This analysis suggests that some active groups were favored at similar hours during both days, e.g., *Opitutus* during the morning (7:00 h), *Rubrimonas* (13:00–16:00 h) in the sediment. During day 2 OTUs are mainly related with cyanobacteria, e.g., *Oscillatoria*, unknown Subcluster III (Fig. 8). In addition, during day 2, methanogens were enriched in the sediments (morning and night) and the water of the pond (Fig. 8). In the water, *Methanomicrobia* and *Methanosarcina* increased their contribution at similar hours as CH_4 and N_2O accumulation was determined in sediment chambers, and other functional groups such as nitrifiers and methane oxidizers were also present (Fig. S5, Fig. S6). SIMPER analyses considering days as factor indicated that archaea associated with single OTUs Nanoarchaeaota (Woesearchaeia), Verrucomicrobia and Bacteroidetes phyla contributed to a higher percentage of the dissimilarity between days in the pond water and sediment (Table S7). These results agreed with previously published studies associated with diel cycles from hypersaline microbial mats from Lake Tyrrel (Australia), showing significant day-night changes associated with Archaea (Nanohaloarchaea) and Bacteroidetes, using metagenomics and lipids analyses (Andrade et al., 2015). During our study, as discussed in Section 3.2, the in-situ microbial activity measured through leucine incorporation are also indicative of a high archaeal growth in the pond associated with higher nitrogen availability as DON compared with other aquatic ecosystems (Batanero et al., 2020). However, Nanoarchaeaota has been characterized as an ectosymbiont of different Crenarchaeotal hosts such as Ignicoccus,

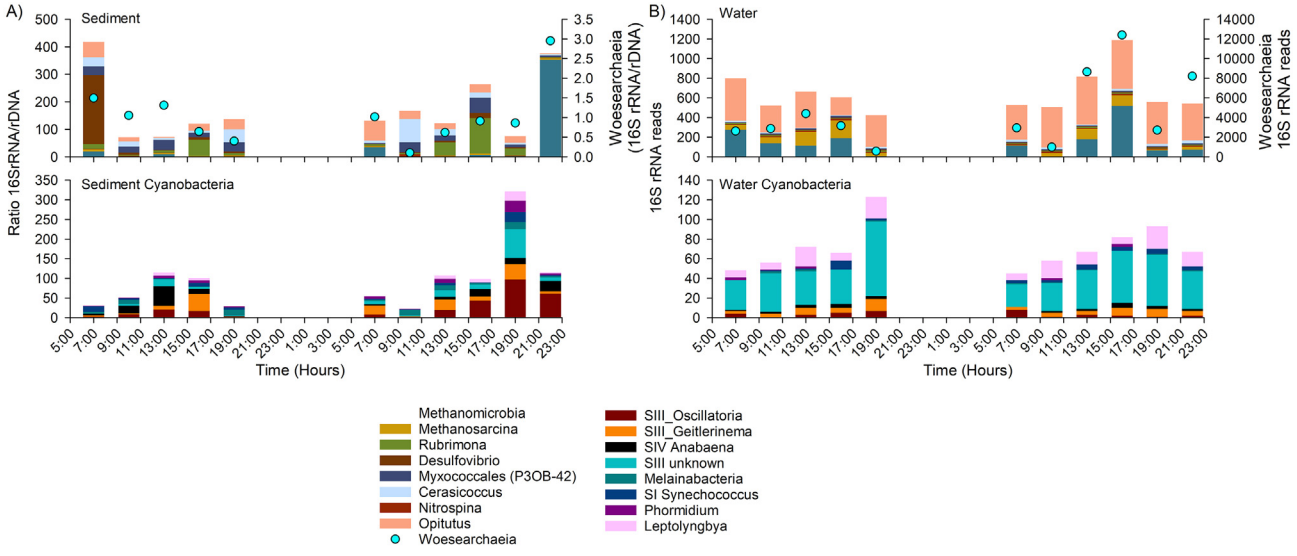

Fig. 8. A) 16S rRNA versus 16S rDNA ratios of sediment microbial community and B) their water counterparts determined using 16S rRNA.

Sulfolobales and Acidilobus, from hydrothermal environments (Munson-McGee et al., 2015; Wurch et al., 2016). Nanoarchaeaota have been recently detected in mesophilic ecosystems including, for example, freshwater lakes from boreal ecosystems (Juottonen et al., 2020) and they are the second most abundant prokaryote on earth according to the Global Prokaryotic Census (Louca et al., 2019). None of the above-mentioned potential hosts from thermal systems were detected during this study, thus a different host is expected in the pond, favored by the conditions observed during the second diel cycle. These biological interactions should be further explored in this extreme ecosystem.

In general, the microbial communities retrieved here were comparable with previously reported studies of evaporitic ponds using different sequencing methods (Eissler et al., 2019) reviewed recently (Dorador et al., 2020). Among the phyla and OTUs exhibiting significant activities showing changes between the two days were Verrucomicrobia, Rhodobacterales and Nanoarchaeota, widespread microbes but potentially enriched in extreme ecosystems. Verrucomicrobia have been characterized as a versatile microbe able to degrade complex polymers and some having nitrogen fixation traits based on metagenome assembled genomes including a recently reported candidate from terrestrial subsurface shale (Nixon et al., 2019). Rhodobacterales are a keystone potential photoheterotrophic group in the wetland (Dorador et al., 2020), where *Rubrimonas* was a significant active group in the sediments during the diel cycle. An isolate from this genus from the Clifton saline lake in Australia was characterized to produce bacteriochlorophyll *a*erobically (Suzuki et al., 1999). Rhodobacterales, Cyanobacteria and Verrucomicrobia could contribute with CO_2 and N_2O sink in the pond, considering their versatile metabolic capabilities, i.e., able to fix CO_2 and use N_2O as electron donor through denitrification in aquaculture ponds (Kathiravan and Krishnani, 2014) or by assimilative pathways in some diazotrophic Cyanobacteria (Cornejo et al., 2015). The microbial processes mitigating CO_2 and N_2O fluxes in the wetland pond and other natural and manmade pond systems (e.g., Table S4) should be further characterized.

In summary, ponds represent a significant landscape in the high-altitude wetland ecosystem. The two diel cycles in the wetland were characterized by abrupt changes in meteorological conditions such as solar radiation, temperature, and wind velocity through the day and between the two days sampled. The second day had a lower solar radiation dose (<1597 W h m^{-2}) before noon, higher temperature, and windier conditions. CO_2 and N_2O gases were more sensitive to these changes, whereas CH_4 was constantly accumulated in the water. The variability in CO_2 and nutrients were associated with photosynthesis and respiration microbial processes in the pond. Over the diel cycle, the pond acted as a net sink of CO_2 and N_2O and a source of CH_4 to the atmosphere. The microbial community was richer in the sediment compared with the water of the pond. The sediment was enriched in key functional groups relative to the water, including photoautotrophs, methanogens and nitrifying bacteria and archaea, these latter covaried with the accumulation of CH_4 and N_2O. The relative contribution of archaea versus bacteria in the total microbial community composition differed between the diel cycles, and the archaea secondary productivity was dominant in the pond water during the second day.

4. Conclusion

The high-altitude wetland pond system presented a biogeochemical dynamic associated with diel changes, including intense nutrient, dissolved organic nitrogen/phosphorus and greenhouse gases recycling, correlated with environmental variables, such as, solar radiation, air temperature and wind velocity. These conditions were associated with the microbial community structure and the activity of specific groups in the sediment and water of the pond, responding to weather and bottom-up, i.e., substrate availability over the two consecutive days of our study. Moreover, our study indicates that high-altitude ponds represent a significant landscape, contributing to the sink of CO_2 and N_2O as other natural and manmade ponds globally and contribute to the understanding of the fine-scale diel variability. Since we cannot predict the same patterns will be present if this field sampling would have continued in time, the higher complexity of high-altitude wetland ecosystems including heterogeneous ponds should be further studied. This would allow us to identify the consistency of the pulses of CH_4 and N_2O excess at hours of high radiation, and determine its relevance compared with other potential carbon buried processes such as sedimentation in this ecosystem. This is extremely important considering that high-altitude wetlands are a reservoir of unknown microbial diversity which metabolisms can influence the recycling and balance of organic matter and energy in these ecosystems.

CRediT authorship contribution statement

Verónica Molina: Conceptualization, Investigation, Formal analysis, Writing - original draft, Project administration, Funding acquisition, Visualization, Resources. **Yoanna Eissler:** Investigation, Formal analysis, Writing - original draft, Visualization. **Camila Fernandez:** Conceptualization, Funding acquisition, Investigation, Resources, Writing - review & editing. **Marcela Cornejo-D'Ottone:** Investigation, Formal analysis, Methodology, Resources, Writing - review & editing. **Cristina Dorador:** Conceptualization, Project administration, Resources, Funding acquisition, Writing - review & editing. **Brad M. Bebout:** Formal analysis, Investigation, Writing - review & editing. **Wade H. Jeffrey:** Formal analysis, Investigation, Writing - review & editing. **Carlos Romero:** Formal analysis, Methodology. **Martha Hengst:** Writing - review & editing.

Declaration of competing interest

The authors declare that they have no known competing financial interests or personal relationships that could have appeared to influence the work reported in this paper.

Acknowledgements

We are grateful to María Jesús Gálvez and Angel Rain for their technical support, to all the participants of the field trip and particularly to Pedro and Margarita Luca for their hospitality at Salar de Huasco shelter facilities. Alejandro Murillo and Klaudia Hernández for helping with H_2S chemical and secondary productivity analyses, respectively. We thank Lomic UMR 7621 for help in dissolved organic matter analysis. This research was funded by FONDECYT, grants numbers 1171324, 1181773, 1180954, 1140356 and Laboratorio Internacional Asociado-Marine Biogeochemistry and Functional Ecology/Multiscale Adaptive Strategies (LIA-MORFUN/MAST).

Appendix A. Supplementary data

Supplementary data to this article can be found online at https://doi.org/10.1016/j.scitotenv.2020.144370.

References

Aguilar, P., Acosta, E., Dorador, C., Sommaruga, R., 2016. Large differences in bacterial community composition among three nearby extreme waterbodies of the high Andean plateau. Front. Microbiol. 7. https://doi.org/10.3389/fmicb.2016.00976.

Anderson, M.J., Gorley, R.N., Clarke, K.R., 2008. PERMANOVA+ for PRIMER: Guide to Software and Statistical Methods, Plymouth, UK. PRIMER-ELtd, Plymouth.

Andrade, K., Logemann, J., Heidelberg, K.B., Emerson, J.B., Comolli, L.R., Hug, L.A., Probst, A.J., Keillar, A., Thomas, B.C., Miller, C.S., Allen, E.E., Moreau, J.W., Brocks, J.J., Banfield, J.F., 2015. Metagenomic and lipid analyses reveal a diel cycle in a hypersaline microbial ecosystem. ISME J. 9, 2697–2711. https://doi.org/10.1038/ismej.2015.66.

Atlas, E.L., Gordon, L.I., Hager, S.W., Park, P.K., 1971. A Practical Manual for use of the Technicon AutoAnalyzer in Seawater Nutrient Analyses (Revised), Tech. Rep. 215. Department of Oceanography, School of Science, Oregon State University, Corvallis, OR, USA.

Barba, J., Poyatos, R., Vargas, R., 2019. Automated measurements of greenhouse gases fluxes from tree stems and soils: magnitudes, patterns and drivers. Sci. Rep. 9, 1–13. https://doi.org/10.1038/s41598-019-39663-8.
Barrett, B.S., Campos, D.A., Veloso, J.V., Rondanelli, R., 2016. Extreme temperature and precipitation events in march 2015 in central and northern Chile. J. Geophys. Res. Atmos. 121, 4563–4580. https://doi.org/10.1002/2016JD024835.
Batanero, G., Green, A., Amat, J., Vittecoq, M., Suttle, C., Reche, I., 2020. Alternation of heterotrophic bacterial and archaeal production along nitrogen and salinity gradients in coastal wetlands. Biogeosci. Discuss., 1–35 https://doi.org/10.5194/bg-2020-60.
Bebout, B.M., Fitzpatrick, M.W., Paerl, H.W., 1993. Identification of the sources of energy for nitrogen fixation and physiological characterization of nitrogen-fixing members of a marine microbial mat community. Appl. Environ. Microbiol. 59, 1495–1503. https://doi.org/10.1128/aem.59.5.1495-1503.1993.
Bunse, C., Pinhassi, J., 2017. Marine Bacterioplankton seasonal succession dynamics. Trends Microbiol. 25, 494–505. https://doi.org/10.1016/j.tim.2016.12.013.
Campbell, B.J., Yu, L., Heidelberg, J.F., Kirchman, D.L., 2011. Activity of abundant and rare bacteria in a coastal ocean. Proc. Natl. Acad. Sci. U. S. A. 108, 12776–12781. https://doi.org/10.1073/pnas.1101405108.
Canfield, D.E., Des Marais, D.J., 1993. Biogeochemical cycles of carbon, sulfur, and free oxygen in a microbial mat. Geochim. Cosmochim. Acta 57 (16), 3971–3984. https://doi.org/10.1016/0016-7037(93)90347-Y.
Cline, J.D., 1969. 14. Spectrophotometric Determination of Hydrogen Sulfide in Natural Waters, pp. 454–458 https://doi.org/10.4319/lo.1969.14.3.0454.
Cornejo, M., Murillo, A.A., Farías, L., 2015. An unaccounted for N2O sink in the surface water of the eastern subtropical South Pacific: physical versus biological mechanisms. Progress in Oceanography 137 (Part a), 12–23. https://doi.org/10.1016/j.pocean.2014.12.016.
Dorador, C., Vila, I., Witzel, K.P., Imhof, J.F., 2013. Bacterial and archaeal diversity in high altitude wetlands of the Chilean Altiplano. Fundam. Appl. Limnol. 182, 135–159. https://doi.org/10.1127/1863-9135/2013/0393.
Dorador, C., Molina, V., Hengst, M., Eissler, Y., Cornejo, M., Fernández, C., Pérez, V., 2020. Microbial communities composition, activity, and dynamics at Salar de Huasco: a polyextreme environment in the Chilean Altiplano. In: Farías, M.E. (Ed.), Microbial Ecosystems in Central Andes Extreme Environments. Springer International Publishing, pp. 123–139 https://doi.org/10.1007/978-3-030-36192-1.
Downing, J.A., Prairie, Y.T., Cole, J.J., Duarte, C.M., Tranvik, L.J., Striegl, R.G., McDowell, W.H., Kortelainen, P., Caraco, N.F., Melack, J.M., Middelburg, J.J., 2006. The global abundance and size distribution of lakes, ponds, and impoundments. Limnol. Oceanogr. 51. https://doi.org/10.4319/lo.2006.51.5.2388.
Edgar, R.C., Haas, B.J., Clemente, J.C., Quince, C., Knight, R., 2011. UCHIME improves sensitivity and speed of chimera detection. Bioinformatics 27, 2194–2200. https://doi.org/10.1093/bioinformatics/btr381.
Eissler, Y., Gálvez, M.J., Dorador, C., Hengst, M., Molina, V., 2019. Active microbiome structure and its association with environmental factors and viruses at different aquatic sites of a high-altitude wetland. Microbiologyopen 8, 1–13. https://doi.org/10.1002/mbo3.667.
Figueroa, F.L., Conde-Álvarez, R., Bonomi Barufi, J., Celis-Plá, P.S., Flores, P., Malta, E.J., Stengel, D.B., Meyerhoff, O., Pérez-Ruzafa, A., 2014. Continuous monitoring of in vivo chlorophyll a fluorescence in ulva rigida (Chlorophyta) submitted to different CO_2, nutrient and temperature regimes. Aquat. Biol. 22, 195–212. https://doi.org/10.3354/ab00593.
de la Fuente, A., 2014. Heat and dissolved oxygen exchanges between the sediment and water column in a shallow salty lagoon. J. Geophys. Res. Biogeosciences 119, 596–613. https://doi.org/10.1002/2013JG002413.
Fuhrman, J.A., Cram, J.A., Needham, D.M., 2015. Marine microbial community dynamics and their ecological interpretation. Nat. Rev. Microbiol. 13, 133–146. https://doi.org/10.1038/nrmicro3417.
Grinham, A., Albert, S., Deering, N., Dunbabin, M., Bastviken, D., Sherman, B., Lovelock, C.E., Evans, C.D., 2018. The importance of small artificial water bodies as sources of methane emissions in Queensland, Australia. Hydrol. Earth Syst. Sci. 22, 5281–5298. https://doi.org/10.5194/hess-22-5281-2018.
He, G., Li, K., Liu, X., Gong, Y., Hu, Y., 2014. Fluxes of methane, carbon dioxide and nitrous oxide in an alpine wetland and an alpine grassland of the Tianshan Mountains, China. J.Arid Land 6 (2014), 717–724. https://doi.org/10.1007/s40333-014-0070-0.
Hernández, K.L., Yannicelli, B., Olsen, L.M., Dorador, C., Menschel, E.J., Molina, V., Remonsellez, F., Hengst, M.B., Jeffrey, W.H., 2016. Microbial activity response to solar radiation across contrasting environmental conditions in Salar de Huasco, northern Chilean altiplano. Front. Microbiol. 7, 1–13. https://doi.org/10.3389/fmicb.2016.01857.
Holmes, R.M., Aminot, A., Kérouel, R., Hooker, B.A., Peterson, B.J., 1999. A simple and precise method for measuring ammonium in marine and freshwater ecosystems. Can. J. Fish. Aquat. Sci. 56, 1801–1808. https://doi.org/10.1139/f99-128.
Hörnlein, C., Confurius-Guns, V., Stal, L.J., Bolhuis, H., 2018. Daily rhythmicity in coastal microbial mats. npj Biofilms Microbiomes. 4, pp. 1–11. https://doi.org/10.1038/s41522-018-0054-5.
Houston, J., 2006. Variability of precipitation in the Atacama Desert: its causes and hydrological impact. Int. J. Climatol. 26, 2181–2198. https://doi.org/10.1002/joc.1359.
Huang, C.-M., Yuan, C.-S., Yang, W.-B., Yang, L., 2019. Temporal variations of greenhouse gas emissions and carbon sequestration and stock from a tidal constructed mangrove wetland. Mar. Pollut. Bull. 149, 110568. https://doi.org/10.1016/j.marpolbul.2019.110568.
Jansson, B.P.M., Malandrin, L., Johansson, H.E., 2000. Cell cycle arrest in archaea by the hypusination inhibitor N(1)-guanyl-1,7-diaminoheptane. J. Bacteriol. 182, 1158–1161. https://doi.org/10.1128/JB.182.4.1158-1161.2000.
Johnson, C.H., Egli, Martin, 2014. Metabolic compensation and circadian resilience in prokaryotic cyanobacteria. Annu. Rev. Biochem. 83, 221–247. https://doi.org/10.1146/annurev-biochem-060713-035632. Metabolic.
Juottonen, H., Fontaine, L., Wurzbacher, C., Drakare, S., Peura, S., Eiler, A., 2020. Archaea in boreal Swedish lakes are diverse, dominated by Woesearchaeota and follow deterministic community assembly. Environ. Microbiol. 00. https://doi.org/10.1111/1462-2920.15058.
Kathiravan, V., Krishnani, K.K., 2014. Diversity of denitrifying bacteria in the greenwater system of coastal aquaculture. Int Aquat Res 6, 135–145. https://doi.org/10.1007/s40071-014-0074-6).
Kuipers, B., Van Noort, G.J., Vosjan, J., Herndl, G.J., 2000. Diel periodicity of bacterioplankton in the euphotic zone of the subtropical Atlantic Ocean. Mar. Ecol. Prog. Ser. 201, 13–25. https://doi.org/10.3354/meps201013.
Levipan, H.A., Quiñones, R.A., Urrutia, H., 2007. A time series of prokaryote secondary production in the oxygen minimum zone of the Humboldt current system, off Central Chile. Prog. Oceanogr. 75, 531–549. https://doi.org/10.1016/j.pocean.2007.08.029.
Long, S.P., Humphries, S., Falkowski, P.G., 1994. Photoinhibition of photosynthesis in nature. Annu. Rev. Plant Physiol. Plant Mol. Biol. 45, 633–662.
Löscher, C.R., Kock, A., Könneke, M., LaRoche, J., Bange, H.W., Schmitz, R.A., 2012. Production of oceanic nitrous oxide by ammonia-oxidizing archaea. Biogeosciences 9, 2419–2429. https://doi.org/10.5194/bg-9-2419-2012.
Louca, S., Mazel, F., Doebeli, M., Parfrey, L.W., 2019. A census-based estimate of earth's bacterial and archaeal diversity. PLoS Biol. 17, 1–30. https://doi.org/10.1371/journal.pbio.3000106.
Loza-Correa, M., Gomez-Valero, L., Buchrieser, C., 2010. Circadian clock proteins in prokaryotes: hidden rhythms? Front. Microbiol. 1, 1–11. https://doi.org/10.3389/fmicb.2010.00130.
Marie, D., Partensky, F., Jacquet, S., Vaulot, D., 1997. Enumeration and cell cycle analysis of natural populations of marine picoplankton by flow cytometry using the nucleic acid stain SYBR green I. Appl. Environ. Microbiol. 63, 186–193. https://doi.org/10.1111/j.1365-294X.2009.04480.x.
McAuliffe, C., 1971. Gas chromatographic determination of solutes by multiple phase equilibrium. Chemical Technology. Chem. Technol. 1, 46–51.
Molina, V., Hernández, K., Dorador, C., Eissler, Y., Hengst, M., Pérez, V., Harrod, C., 2016. Bacterial active community cycling in response to solar radiation and their influence on nutrient changes in a high-altitude wetland. Front. Microbiol. 7. https://doi.org/10.3389/fmicb.2016.01823.
Molina, V., Dorador, C., Fernández, C., Bristow, L., Eissler, Y., Hengst, M., Hernandez, K., Olsen, L.M., Harrod, C., Marchant, F., Anguita, C., Cornejo, M., 2018a. The activity of nitrifying microorganisms in a high-altitude Andean wetland. FEMS Microbiol. Ecol. 94, 1–13. https://doi.org/10.1093/femsec/fiy062.
Molina, V., Eissler, Y., Cornejo, M., Galand, P.E., Dorador, C., Hengst, M., Fernandez, C., Francois, J.P., 2018b. Distribution of greenhouse gases in hyper-arid and arid areas of northern Chile and the contribution of the high altitude wetland microbiome (Salar de Huasco, Chile). Antonie van Leeuwenhoek. Int. J. Gen. Mol. Microbiol. 111, 1421–1432. https://doi.org/10.1007/s10482-018-1078-9.
Munson-McGee, J.H., Field, E.K., Bateson, M., Rooney, C., Stepanauskas, R., Young, J., 2015. Distribution across Yellowstone National Park Hot Springs. Appl. Environ. Microbiol. 81, 7860–7868. https://doi.org/10.1128/AEM.01539-15.Editor.
Needham, D.M., Chow, C.E.T., Cram, J.A., Sachdeva, R., Parada, A., Fuhrman, J.A., 2013. Short-term observations of marine bacterial and viral communities: patterns, connections and resilience. ISME J. 7, 1274–1285. https://doi.org/10.1038/ismej.2013.19.
Nixon, S.L., Daly, R.A., Borton, M.A., Solden, L.M., Welch, S.A., Cole, D.R., Mouser, P.J., Wilkins, M.J., Wrighton, K.C., 2019. Genome-resolved metagenomics extends the environmental distribution of the verrucomicrobia phylum to the deep terrestrial subsurface. mSphere 4, 1–18. https://doi.org/10.1128/msphere.00613-19.
Prelle, L.R., Graiff, A., Gründling-Pfaff, S., Sommer, V., Kuriyama, K., Karsten, U., 2019. Photosynthesis and respiration of Baltic Sea benthic diatoms to changing environmental conditions and growth responses of selected species as affected by an adjacent peatland (Hütelmoor). Front. Microbiol. 10, 1–19. https://doi.org/10.3389/fmicb.2019.01500.
Pujopay, M., Raimbault, P., 1994. Improvement of the wet-oxidation procedure for simultaneous determination of particulate organic nitrogen and phosphorus collected on filters. Mar. Ecol. Prog. Ser. 105, 203–207. https://doi.org/10.3354/meps105203.
Quast, C., Pruesse, E., Yilmaz, P., Gerken, J., Schweer, T., Yarza, P., Peplies, J., Glöckner, F.O., 2013. The SILVA ribosomal RNA gene database project: improved data processing and web-based tools. Nucleic Acids Res. 41, D590–D596.
Sawall, Y., Hochberg, E.J., 2018. Diel versus time-integrated (daily) photosynthesis and irradiance relationships of coral reef organisms and communities. PLoS One 13, 1–13. https://doi.org/10.1371/journal.pone.0208607.
Schloss, P.D., Westcott, S.L., Ryabin, T., Hall, J.R., Hartmann, M., Hollister, E.B., Lesniewski, R.A., Oakley, B.B., Parks, D.H., Robinson, C.J., Sahl, J.W., Stres, B., Thallinger, G.G., Van Horn, D.J., Weber, C.F., 2009. Introducing mothur: open-source, platform-independent, community-supported software for describing and comparing microbial communities. Appl. Environ. Microbiol. 75, 7537–7541. https://doi.org/10.1128/AEM.01541-09.
Shade, A., Jones, S.E., Caporaso, J.G., Handelsman, J., Knight, R., Fierer, N., Gilbert, J.A., 2014. Conditionally rare taxa disproportionately contribute to temporal changes in microbial diversity. Microb. Divers. 5, 1–9. https://doi.org/10.1128/mBio.01371-14.
Siljanen, H.M.P., Alves, R.J.E., Ronkainen, J.G., Lamprecht, R.E., Bhattarai, H.R., Bagnoud, A., Marushchak, M.E., Martikainen, P.J., Schleper, C., Biasi, C., 2019. Archaeal nitrification is a key driver of high nitrous oxide emissions from arctic peatlands. Soil Biol. Biochem. 137, 107539. https://doi.org/10.1016/j.soilbio.2019.107539.
Simon, M., Azam, F., 1989. Protein content and protein synthesis rates of planktonic marine bacteria. Mar. Ecol. Prog. Ser. 51, 201–213. https://doi.org/10.3354/meps051201.
Smith, J.M., Chavez, F.P., Francis, C.A., 2014. Ammonium uptake by phytoplankton regulates nitrification in the sunlit ocean. PLoS One 9. https://doi.org/10.1371/journal.pone.0108173.

Smith, S.V., Renwick, W.H., Bartley, J.D., Buddemeier, R.W., 2002. Distribution and significance of small, artificial water bodies across the United States landscape. Sci Total Environ 299, 21–36. https://doi.org/10.1016/S0048-9697(02)00222-X.

Squeo, F.A., Warner, B.G., Aravena, R., Espinoza, D., 2006. Bofedales: high altitude peatlands of the Central Andes. Rev. Chil. Hist. Nat. 79, 245–255. https://doi.org/10.4067/S0716-078X2006000200010.

Stal, L.J., Heyer, H., 1987. Dark anaerobic nitrogen fixation (acetylene reduction) in the cyanobacterium Oscillatoria sp. FEMS Microbiol. Lett. 45, 227–232. https://doi.org/10.1016/0378-1097(87)90056-5.

Suzuki, T., Muroga, Y., Takahama, M., Shiba, T., Nishimura, Y., 1999. Rubrimonas cliftonensis gen. nov., sp. nov., an aerobic bacteriochlorophyll-containing bacterium isolated from a saline lake. Int. J. Syst. Bacteriol. 49, 201–205. https://doi.org/10.1099/00207713-49-1-201.

Tokida, T., Miyazaki, T., Mizoguchi, M., Seki, K., 2005. In situ accumulation of methane bubbles in a natural wetland soil. Eur. J. Soil Sci. 56, 389–396. https://doi.org/10.1111/j.1365-2389.2004.00674.x.

Torgersen, T., Branco, B., 2008. Carbon and oxygen fluxes from a small pond to the atmosphere: temporal variability and the CO_2/O_2 imbalance. Water Resour. Res. 44, 1–14. https://doi.org/10.1029/2006WR005634.

Wang, Q., Zhang, L., Shen, J., Du, S., Han, L.-L., He, J.-Z., 2016. Nitrogen fertiliser-induced changes in N2O emissions are attributed more to ammonia-oxidising bacteria rather than archaea as revealed using 1-octyne and acetylene inhibitors in two arable soils. Biol. Fertil. Soils 52, 1163–1171. https://doi.org/10.1007/s00374-016-1151-3.

Wuebbles, D.J., Hayhoe, K., 2002. Atmospheric methane and global change. 57, pp. 177–210. https://doi.org/10.1007/978-94-015-9343-4_1.

Wurch, L., Giannone, R.J., Belisle, B.S., Swift, C., Utturkar, S., Hettich, R.L., Reysenbach, A.L., Podar, M., 2016. Genomics-informed isolation and characterization of a symbiotic Nanoarchaeota system from a terrestrial geothermal environment. Nat. Commun. 7. https://doi.org/10.1038/ncomms12115.

Yates, C.A., Johnes, P.J., Owen, A.T., Brailsford, F.L., Glanville, H.C., Evans, C.D., Marshall, M.R., Jones, D.L., Lloyd, C.E.M., Jickells, T., Evershed, R.P., 2019. Variation in dissolved organic matter (DOM) stoichiometry in U.K. freshwaters: assessing the influence of land cover and soil C:N ratio on DOM composition. Limnol. Oceanogr. 64, 2328–2340. https://doi.org/10.1002/lno.11186.

Zhu, Y., Purdy, K.J., Eyice, Ö., Shen, L., Harpenslager, S.F., Yvon-Durocher, G., Dumbrell, A.J., Trimmer, M., 2020. Disproportionate increase in freshwater methane emissions induced by experimental warming. Nat. Clim. Chang. 10 (2020), 685–690. https://doi.org/10.1038/s41558-020-0824-y.